

# Structural and microstructural properties of porous PZT films

V. STANCU<sup>a\*</sup>, I. BOERASU<sup>c</sup>, M. LISCA<sup>a</sup>, L. PINTILIE<sup>b</sup>, M. POPESCU<sup>a</sup>, F. SAVA<sup>a</sup>

<sup>a</sup> National Institute of Materials Physics Bucharest-Magurele, P. O. Box MG-7, 77125, Romania

<sup>b</sup> Max Planck Institute of Microstructure Physics, Weinberg 2, Halle, 06129 Germany

<sup>c</sup> Josef Stefan Institute, Jamova 39, 1000 Ljubljana, Slovenia

PbZr<sub>1-x</sub>Ti<sub>x</sub>O<sub>3</sub> (PZT) film was prepared by addition of polymer polyvinylpyrrolidone (PVP) in the PZT precursor and hydrolysis of the PZT precursor sol. Porous thin films were prepared by spin coating on Pt-coated Si substrate. The structure of the films was investigated by X-ray diffraction (XRD). (100)-oriented PZT 20/80 film was obtained by hydrolysis of sol. PVP addition leads to the (110)-orientation of the film. The surface microstructure of the films was characterised with Atomic Force Microscopy (AFM) and Scanning Electron Microscopy (SEM). The surface profile indicates a films roughness of 5 nm. No micro-cracks were observed on film surface. The average remnant polarization and the coercive field were obtained from the hysteresis loop measurements. The ferroelectric behavior has been evidenced by the presence of the butterfly shape of the capacitance-voltage characteristics. Experimental results show that the dielectric constant of the PZT porous film is lower than that of the dense film.

(Received June 8, 2006; accepted July 20, 2006)

**Keywords:** Porous PZT films, Polyvinylpyrrolidone (PVP), Hydrolysis

## 1. Introduction

During recent years a considerable attention was given to the use of ferroelectric thin films of the PbZr<sub>1-x</sub>Ti<sub>x</sub>O<sub>3</sub> (PZT) family for memory, piezoelectric and pyroelectric devices. Thin films are good candidate materials because of their remarkable ferroelectric, piezoelectric and pyroelectric [1] properties. Pyroelectric thin films have many applications in temperature sensing systems for fire and intruder detection, air condition control and thermal imaging [2]. PZT 20/80 films are ideal for pyroelectric applications, involving detection of IR radiation. However, to increase the voltage response ( $F_v = p / \epsilon_r$ ) it is necessary not only to maximise the pyroelectric coefficient,  $p = \Delta P_s / \Delta T$ , but to lower the dielectric permittivity as well. A possible way to decrease the characteristic value of dielectric constant of PZT 20/80 is to incorporate pores into the material structure.

A number of fabrication processes have been developed for the fabrication of PZT films including organo-metallic chemical vapour deposition [3], sputtering [4], ion-beam deposition [5] and sol-gel method [6,7]. Among these methods, the sol-gel process offers several advantages including easy control of chemical composition, good stoichiometry, high purity and lower processing temperatures. The most widely used sol-gel route for PZT thin film fabrication is the methoxyethanol route demonstrated by Budd et al. [6]. This route requires dry atmosphere processing conditions in order to avoid uncontrolled hydrolysis of Ti and Zr alkoxides. These methods have been modified over the years [8,9]. Ti and Zr alkoxides were stabilised by chelating agents or using other alcohol solvents [10-12]. Most of the schemes reported for the sol-gel processing of ferroelectric PZT thin films use hydrated lead precursor Pb(OOCCH<sub>3</sub>)<sub>2</sub>·3H<sub>2</sub>O which requires in situ dehydration by

refluxing in 2-methoxyethanol solvent. Generation of free acid, ester and alcohol causes changes in the chemistry [15] of the precursor solution by inducing premature hydrolysis and precipitation of the more reactive component in a multicomponent system affecting the homogeneity and uniformity of the thin layers. The obtained precursor solution is sensitive to moisture and therefore, the processing is carried out under controlled dry conditions. The addition of drying agent will stabilise the system. The excess organic compounds present in the amorphous gel can cause shrinkage stress in films during thermal processing. [16]

Porosity can be introduced in thin films by controlling the nucleation and growth during thermal annealing of the material or by adding a polymer in the PZT precursor solution prior to spin coating the substrate [13,14,18].

To develop a method for the production of porous film, the initial hydrolysis of the precursor solution and the addition of organic macromolecular polyvinylpyrrolidone (PVP) were tested. In this article we report the preparation of porous films of a PZT and compare their dielectric properties observed with those of PZT dense film.

## 2. Experimental

The stock solution of PbZr<sub>0.2</sub>Ti<sub>0.8</sub>O<sub>3</sub> has been prepared using lead acetate trihydrate, Pb(OOCCH<sub>3</sub>)<sub>2</sub>·3H<sub>2</sub>O, titanium isopropoxide, Ti[OCH(CH<sub>3</sub>)<sub>2</sub>]<sub>4</sub> and zirconium n-propoxide, Zr[OCH<sub>2</sub>CH<sub>2</sub>CH<sub>3</sub>]<sub>4</sub>, as precursor materials. 2-methoxyethanol (2ME), CH<sub>3</sub>OCH<sub>2</sub>CH<sub>2</sub>OH, was used as solvent. A 5wt% PbO excess was added to compensate the Pb evaporation during the crystallization step. Fig. 1 illustrates the experimental flow diagram used for the preparation of stock solution and porous films.

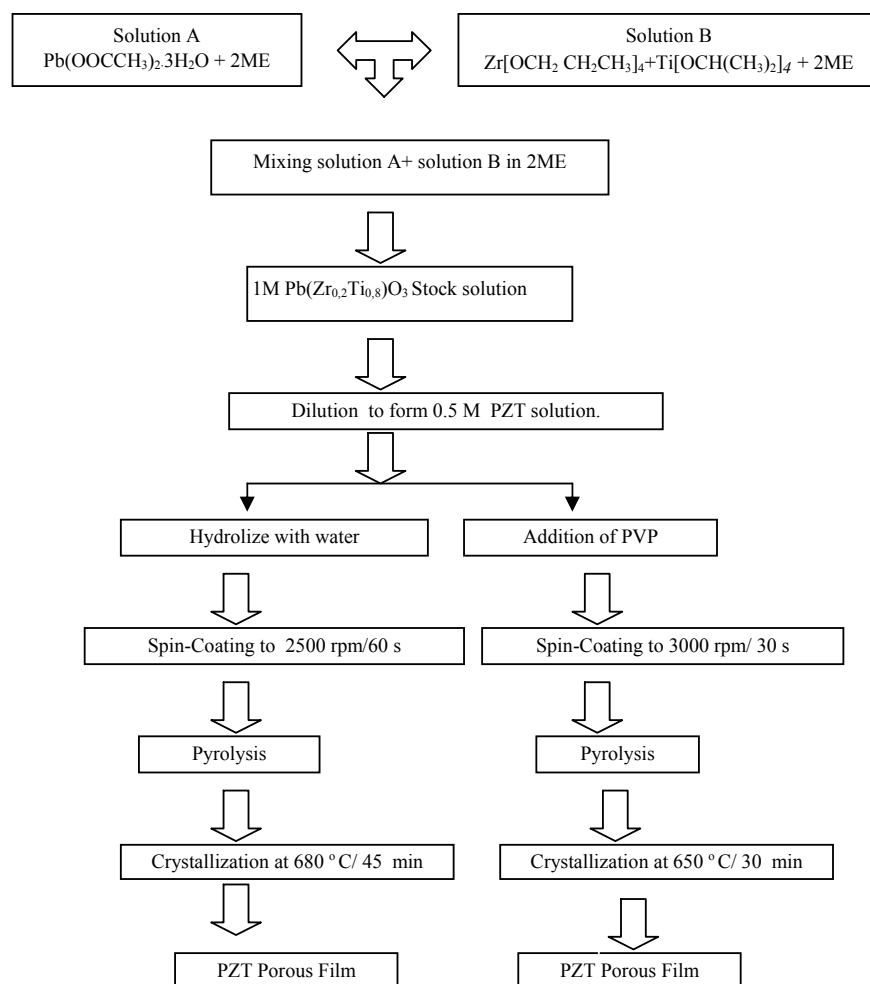


Fig. 1. Flow diagram for the sol-gel processing of PZT porous films.

The lead precursor, was dissolved in 2-methoxyethanol, heated to 110 °C and distilled to remove water. This procedure was repeated two times. The dehydrated solution, i.e. solution A, was cooled to room temperature. The titanium and zirconium precursor, was prepared by mixing titanium isopropoxide and zirconium n-propoxide in 2-methoxyethanol, heated to 110 °C and distilled for two times. The resulting solution, i.e. solution B, was cooled down to room temperature. A convenient stock solution of PZT was prepared by mixing a definite volume of solution A and solution B in 2-methoxyethanol medium. Two distillations were again performed to complete the reaction and remove any remaining reaction by-products. The final Pb/Zr/Ti solution was diluted with 2-methoxyethanol to obtain a 0.5 M stock solution. To improve the porosity formation, the stock solution was: a) hydrolysed in a molar ratio Pb: H<sub>2</sub>O = 1:3 (sample P1) and (b) addition of PVP in 7 wt% (sample P2). The PVP (C<sub>6</sub>H<sub>9</sub>ON) used in experiment has the average molecular weight of 25 000 (Fig. 2). The precursor solution was syringed through a 0.2 mm filter onto Pt-coated Si substrates and spun using a spinner

operating at 2500 rpm for 60s (P1) and 3000 rpm for 30s (P2). After each deposition, a two-step hot plate treatment was then used at 200 °C/ 2 min, 400 °C/ 5 min (P1), at 200 °C/ 2 min and 350 °C/ 5 min (P2), respectively. The sequence coating-thermal treatment was repeated until the desired thickness was obtained.

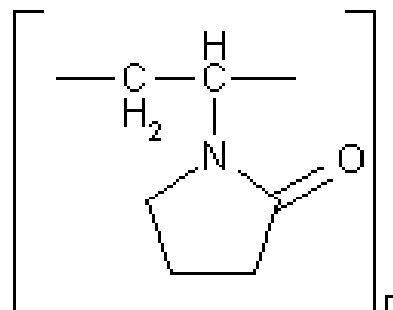


Fig. 2. Schematic illustration to the molecular structure of PVP.

The resulting films were amorphous. The transition from the amorphous structure to the perovskite structure was achieved by placing the samples in a tube-furnace in which the temperature was progressively raised (heating rate of 20 °C/ min and 5 °C/ min, respectively) to the annealing temperature 680 °C/ 45 min (P1) and 650 °C/ 30 min (P2), respectively. To compare the porous films, the sample P3 was deposited in the same condition as P2 without PVP.

The thermal treatment of porous thin films obtained by addition of PVP was chosen according to thermo-differential data (TG/DTA, STA 409C/CD, Netzsch).

The crystalline phases of thin films were identified by X-ray diffraction (XRD) in 2θ geometry. The microstructure of the films were investigated by scanning electron microscopy (SEM) and atomic force microscopy (AFM). Gold electrodes were deposited by thermal evaporation through a shadow mask onto the surface of PZT thin films. The dielectric constant  $\epsilon_r$ , was estimated from room temperature capacitance-voltage (C-V) characteristics obtained from a Agilent LCR meter, for 1 kHz frequency measurement. P-E hysteresis loops were also obtained at 100 Hz using a RT 66A Analyser.

### 3. Results and discussion

#### 3.1. Structural and microstructure analysis

Fig. 3 shows the XRD patterns for the sol-gel derived PZT 20/80 films obtained by (a) hydrolysis of the precursor solution (Pb: H<sub>2</sub>O = 1:3) and (b) addition of PVP (7wt%). The spectra show typical reflection patterns attributed to tetragonal (perovskite) crystal symmetry. Fig. 3 shows that the porous films deposited on Pt-coated Si grow preferentially along the (100) (P1) and (110) (P2) crystallographic directions. For P1 and P2 all diffraction peak corresponding to (100), (101), (111) planes of PZT were obtained. In the X-ray diffraction spectra no peak corresponding to PVP were revealed.

In general, the PZT films deposited on Pt-coated Si grow with a preferential orientation along (111) crystallographic direction. The origin of this effect is usually related to the heterogeneous nucleation which takes place at the film/substrate interface. It was argued in the literature that an intermetallic phase of Pt<sub>x</sub>Pb forms at the interface PZT/Pt in the early stage of sol-gel deposition of PZT films [17]. The intermetallic phase proceeds as a nucleation site for the perovskite phase nuclei that start to grow consuming the pyrochlore phase produced initially. However, this phase is supposed to play a central role not only in the pyrochlore-to-perovskite phase transformation, but also it acts as a lattice-matching buffer layer between the Pt electrode and the PZT 20/80.

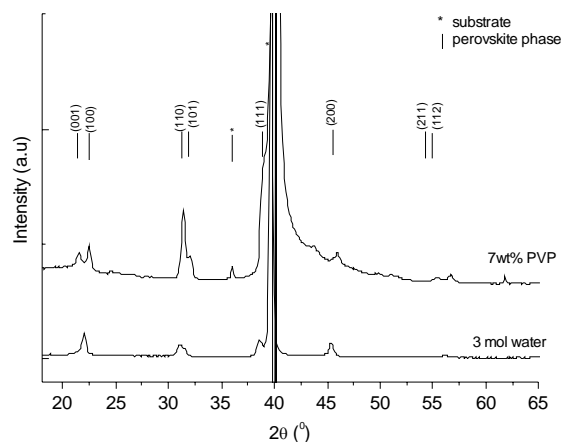
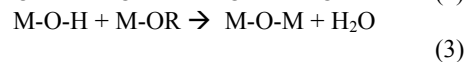
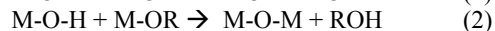


Fig. 3. X-ray diffraction patterns of PZT porous films.

The sol chemistry is based on the hydrolysis and condensation of inorganic salts in metal alkoxides [21]. The advantage of using alkoxides comes from the possibility to control the reaction rate by controlling the hydrolysis and the condensation. The hydrolysis of alkoxide occurs as shown in eq. (1), and condensation of two M-OH groups or reaction of a M-OR with M-OH group is described in eq. (2) and (3):



with M = metal, R = ligand;

Each one of these chemical reactions depend on many parameters such as the nature of the metallic atom M, the nature of the alkyl R group, the concentration, the temperature and the alkoxide/water ratio (r) [21]. In the sol-gel chemistry, the H<sub>2</sub>O is indispensable for the formation of a metal/oxide polymer by a partial hydrolysis and subsequent polymerization of hydrolyzed species. In addition, the water concentration can control both the gelation time and the degree of cross-linking of the polymer.

In this work, the hydrolyzed precursor solution with 3 moles of water/ Pb acetate consists in polymers or macromolecules built of many monomers (-O-M-). Porosity or cavities should develop when either the water or the solvent has been removed during the pyrolysis step. Either surface diffusion or evaporation-condensation processes, that take place on the pores surface, will considerably reduce the energy of the system. In turn, the pore's surface acts as nucleation centre of the perovskite phase. Since the barrier for the nucleation is reduced, the orientation of the film will be controlled by the growth step. For PZT systems, the crystallographic direction with the lowest surface energy was found to be (100) [19].

When PVP is added into the precursor it can hybridize with metalloxane polymer in molecular scale

through strong hydrogen bonding between C = O group of PVP and the OH group of the metalloxane polymer [24]. The C = O group can suppress the condensation reaction and promote the structural relaxation. The pores were produced after the pyrolysis of PVP which was released at high temperature and left pores where it existed before annealing [18].

From the thermal analysis (TG/DTA), we observed that after 550 °C the PVP was eliminated from the PZT-PVP solution (Fig. 4).

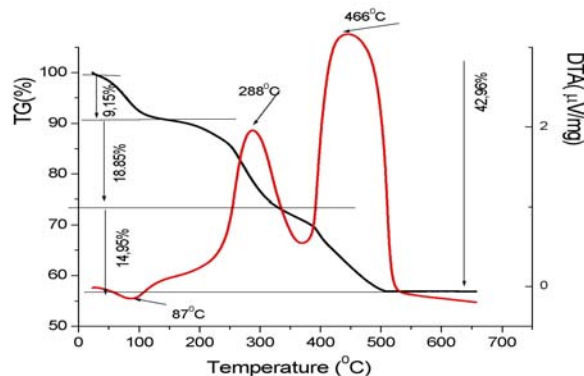


Fig. 4. TG/DTA Analysis of PZT+7wt%PVP dried at 150 °C for 8 h.

The TG analysis of the PZT-PVP precursor solution presented three regions in the investigated temperature range. Up to 550 °C, the total losses of the PZT solution were 42.96 wt%. The DTA curve show one endothermic peak at 88 °C related to the elimination of the weakly bonded water and two exothermal peaks: one around 288 °C, corresponding to the decomposition and combustion of organic substances; second at 446 °C, corresponding to the total elimination of residue and total decomposition of polymer. The major weight loss in the second region is due to the decomposition of the hydroxyl and remaining alkoxide and acetate groups. Usually, the combustion of organics occurs by elimination of water and carbon dioxide. The detected acetone in the evolved gasses is a consequence of the presence of acetate groups which decomposes by a reaction in two steps into acetone, carbon dioxide and oxide. The presence of NO<sub>2</sub> is correlated with the polymer combustion. In the third region the exothermic peak in the DTA with an associated a weight loss where CO<sub>2</sub>, NO<sub>2</sub> is evolved due to the decomposition of probably some carbonates, carbonaceous and polymer residues. After 550 °C no weight loss can be observed, suggesting the decomposition is terminated.

Fig. 5 is a cross-section view by scanning electron microscopy on a fresh fractured sample of porous PZT film deposited on Pt-coated Si. It reveals that a granular and porous microstructure was obtained in the sol-gel derived PZT films obtained by hydrolysis of the precursor solution with 3 moles of water. The porosity is

incorporated and randomly distributed into the perovskite phase. The film deposited consist of ten layers, corresponding to a film thickness of about 600 nm. The porosity of the film obtained by addition of PVP is better defined in comparison with the previous sample.

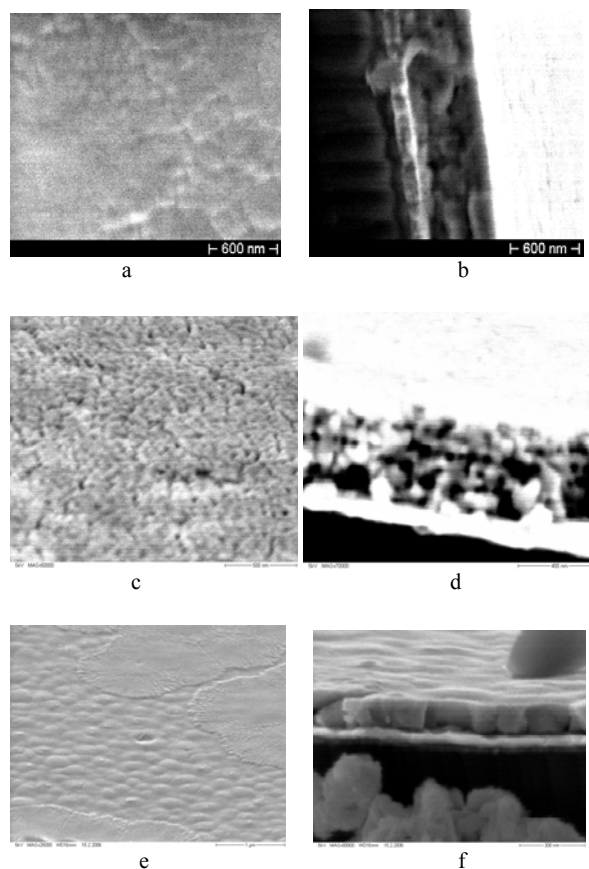


Fig. 5. (a) SEM micrographs of porous PZT film containing 3 mol water (b) cross sectional view of porous PZT film containing 3 mol water (c) SEM micrographs of porous PZT film containing 7wt% PVP (d) cross sectional view of porous PZT film containing 7wt% PVP (e) SEM micrographs of dense PZT film (f) cross sectional view of dense PZT film.

There are no pores going from the top to the bottom of the films. The pores are small and relatively uniformly distributed into the film. The SEM micrographs of the sample with PVP show that the surface contains small surface pores. The estimated thickness of the film with six layers from the SEM micrograph of the cross section was 380 nm. In the case of P sample deposited on Pt/Si some characteristic "rosettes" can be observed. The estimated thickness of the dense film with six layers is 300 nm.

Fig. 6 shows the AFM images of porous PZT films surface. The average crystallite size is around ~ 66 nm for P1 and (b) 85 nm for P2. The corresponding roughness is ~ 4 nm.

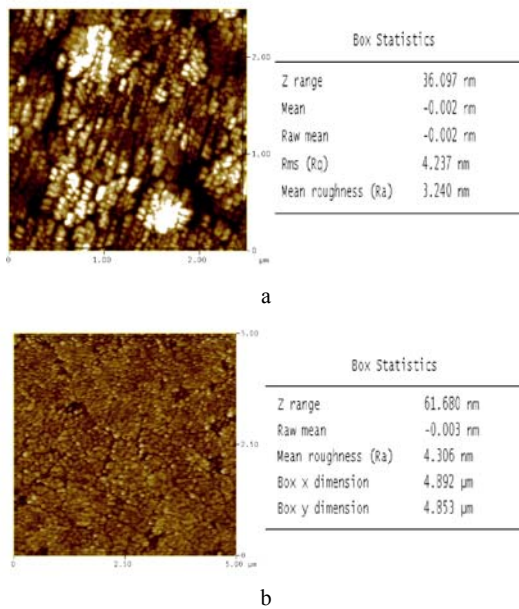


Fig. 6. AFM image of (a) PZT porous thin film containing 3 mol water (P1) (b) PZT porous thin film containing 7wt% PVP (P2).

**3.2. Electrical characterisation**

The ferroelectric loop of the PZT porous film can be seen in Fig. 7. Table 1 shows the average remnant polarization ( $P_r$ ) and the average coercive field ( $E_c$ ) of the investigated films. It is seen that the ferroelectric properties are by far lower than those reported for dense PZT 20/80 films [20]. The calculated coercive field for P1 is low for PZT films in the hydrolysis method. Moreover, the hysteresis curve is asymmetric both along the field and polarization axes, most probable related to the electrodes asymmetry, i.e. different work function. The hysteresis curve for P2 is almost symmetric both along the field and polarization axes.

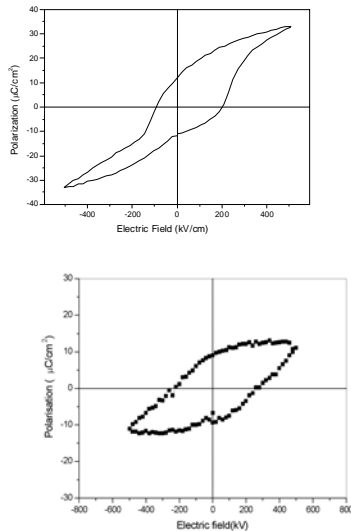


Fig. 7. P-E hysteresis loop for porous PZT 20/80 thin films at 100 Hz and room temperature: (a) P1 (b) P2.

Fig. 8 shows the C-V curve of the porous PZT film. The curve shows a typical butterfly shape. The values of the bias voltage of the two peaks are slightly asymmetric along either the capacitance or voltage axes, most probable related to the electrodes asymmetry.

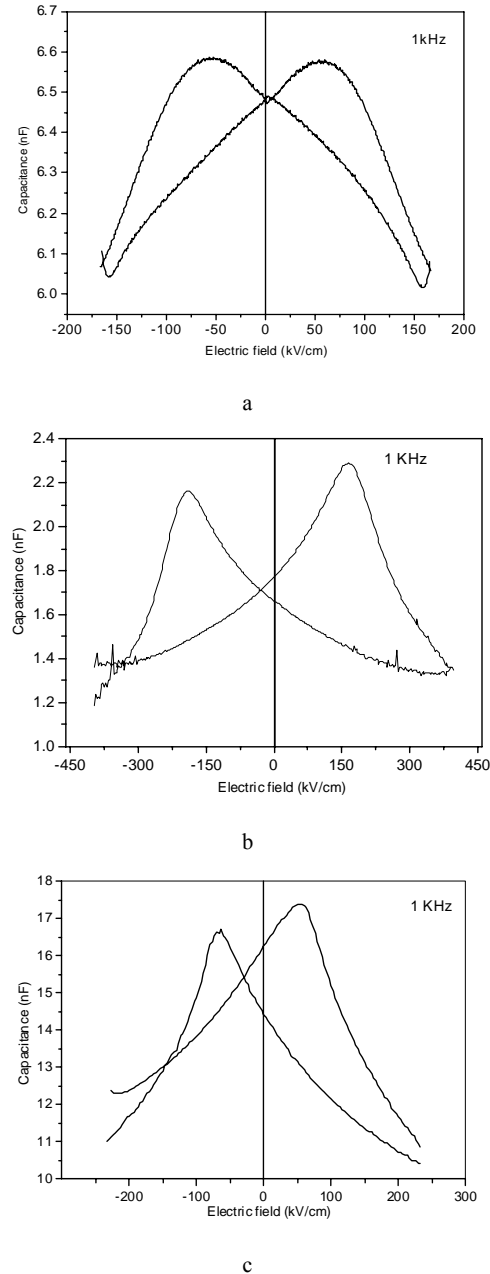


Fig. 8. C-V curves for Au/PZT porous/Pt capacitor at room temperature and 1kHz (a) P1 sample (b) P2 sample (c) PZT dense film.

From the C-V curve, the zero field relative permittivity of porous PZT film was calculated using the model of a plan parallel capacitor. The obtained values are given in Table 2. We compared the permittivity value of porous sample with permittivity value of dense PZT (P3) prepared in our laboratory in the same conditions as the

porous sample. The calculated values of dielectric permittivity of porous films are lower than in PZT dense film.

Table 1. Average  $P_r$  si  $E_c$  values for PZT porous thin film containing 3 mol water (P1) and PZT porous thin film containing 7wt% PVP (P2).

	$P_{r+}$	$P_{r-}$	$P_{rm}$	$E_{c+}$	$E_{c-}$	$E_{cm}$
P1	11. 7	10.9	11.3	126	58	92
P2	9.0	9.3	9.2	250	250	250

Table 2. The dielectric constant and geometrical dimension of PZT 20/80 porous film.

	d (nm)	S (mm <sup>2</sup> )	$\epsilon$
PZT + 3 mol water (P1)	600	1.5	292
PZT + 7wt%PVP (P2)	380	1.5	48
PZT dense (P3)	300	1.5	348

When the considerations are limited to SEM investigation, the deposited porous PZT films resemble as a composite material consisting in PZT grains and pores. If so, the permittivity from Table 2 it is the one of the composite material from which one could to extract the PZT's permittivity. For this purpose, the spherical bubbles model could be applied. One of the most difficult tasks is to estimate the porosity. Even if several procedures of porosity calculation have been reported in the literature [22,23], this topic is still matter of debate. We have used an analytic approach to estimate the amount of porosity in deposited films. Considering that the dielectric permittivity of deposited PZT films is  $\epsilon_{film} = 348$  and is similar to those reported by Klee [20], i.e.  $\epsilon_b = 350$ , then the p coefficient can be estimated. The calculated value is 15% for P1 and 60% for P2.

#### 4. Conclusions

Porous pyroelectric thin films of PZT have been synthesized by hydrolysis of the precursor solution with 3 moles of water and by incorporating a polymer to the precursor solution. It was shown that the addition of polymer induces a better porous microstructure than the hydrolysis of PZT sol. The spherical bubbles model was used to estimate the film porosity. For PZT the porosity values were increased from 15% estimated for sample prepared by initial hydrolysis of PZT precursor solution to 40 % by introducing PVP in the PZT precursor solution. The dielectric permittivity was calculated using the plan parallel capacitor model and it was found to be lower than that for dense films. The dielectric permittivity value decreases from 348 for dense film to 298 and 48 for porous films. This way, the characteristic of pyroelectric materials, the voltage response will increase and porous PZT 20/80 film will be a potential candidate for pyroelectric applications.

#### Acknowledgement

This work was supported by CERES 4-252 "FENAPOFS" Project of the Romanian Ministry of Education and Research.

#### References

- [1] M. Kohli, C. Wuethrich, K. Brooks, B. Willing, M. Forser, M. Muralt, N. Setter, P. Ryser, *Sensor and Actuator A* **60**, 147 (1997).
- [2] R. W. Whatmore, *Rep. Prog. Phys.* **49**, 1335 (1986).
- [3] W. Braun, B. S. Kwak, A. Erbil, J. D. Budai, B. J. Wilkens, *Appl. Phys. Lett* **63**, 467 (1993).
- [4] K. Iijima, Y. Tomita, R. Takayama, I. Ueda, *J. Appl. Phys* **60**, 361 (1986).
- [5] R. N. Castellano, L. G. Feinstein, *J. Appl. Phys* **50**, 4406 (1979).
- [6] K. D. Budd, S. K. Dey, D. A. Payne, *Brit. Ceram. Proc.* **36**, 107 (1985).
- [7] G. Yi, Z. Wu, M. Sayer, *J. Appl. Phys* **64**, 2717 (1988).
- [8] C. D. E. Lakerman, D. A. Payne, *J. AM. Ceram. Soc.* **75**, 3091 (1992).
- [9] L. E. Sanchez, D. T. Dion, S. Y. Wu, I. K. Naik, *Ferroelectrics* **116**, 1-17 (1991).
- [10] S. J. Milne, S. H. Pyke, *J. Am. Ceram. Soc* **74**, 1407 (1991).
- [11] S. J. Chen, A. Janah, J. D. Mackenzie, in *Better Ceramics through Chemistry II*, edited by C. J. Brinker, D. E. Clark and D. R. Ulrich (Mater. Res. Symp. Proc 73, Pittsburg, PA, 1986), P.731.
- [12] N. Tohge, S. Takahashi, T. Minami, *J. Am. Ceram. Soc* **74**, 67 (1991).
- [13] G. Suyal, N. Setter, *J. Eur. Ceram. Soc* **24**, 247 (2004).
- [14] A. Seifert, L. Sagalowicz, P. Muralt, N. Setter, *J. Mat. Res.* **14**, 2012 (1999).
- [15] C. D. E. Lakerman, J. F. Campion, D. A. Payne, *CERAM> Trans.* **25**, 413 (1992).
- [16] V. Kumar, Y. Ohya, Y. Takahashi, *Jpn. J. Appl. Phys.* **37**, 4477 (1998).
- [17] Z. Huang, Q. Zhang, R. W. Whatmore, *J. Appl. Phys* **86**, 1662 (1999).
- [18] Z. Wang, J. Liu, T. Ren, L. Liu, *Sensor and Actuators A* **117**, 293 (2005).
- [19] K. G. Brooks, I. M. Reaney, R. Klissurska, Y. Huang, L. Bursill, N. Setter, *J. Mater. Res.* **9**, 2540 (1994).
- [20] M. Klee, R. Eusemann, R. Waser, W. Brand, H. van Hal, *J. Appl. Phys.* **72**, 1566 (1992).
- [21] C. J. Brinker, G. W. Scherer, *Sol-gel science*, Academic Press, San Diego (1990).
- [22] A. Seifert, P. Muralt, N. Setter, *J. Appl. Phys.* **72**, 2409 (1998).
- [23] Q. Zhang, S. Corkovic, C. P. Shaw, Z. Huang, R. W. Whatmore, *Thin Solid Film* **488**, 258 (2005).
- [24] H. Kozuka, M. Kajimura, *J. Am. Ceram. Soc.* **83**, 1056 (2000).

\* Corresponding author: stancu@infim.ro